

High-power Targetry for Future Accelerators
September 8–12, 2003

Modeling of Free Surface MHD Flows and Cavitation

Roman Samulyak

*Center for Data Intensive Computing
Brookhaven National Laboratory
U.S. Department of Energy*

rosamu@bnl.gov

Brookhaven Science Associates
U.S. Department of Energy

Talk outline

- Theoretical and numerical ideas implemented in the FronTier-MHD, a code for free surface compressible magnetohydrodynamics code.
- Some numerical examples (Simulation related to Neutrino Factory/Muon Collider Target will be discussed in Y. Prykarpatsky's talk).
- Bubbly fluid/cavitation modeling and some benchmark experiments. Possible application for SNS target problems.
- Future plans

The system of equations of compressible magnetohydrodynamics: an example of a coupled hyperbolic – parabolic/elliptic subsystems

$$\frac{\partial \rho}{\partial t} = -\nabla \cdot (\rho \mathbf{u})$$

$$\rho \left(\frac{\partial}{\partial t} + \mathbf{u} \cdot \nabla \right) \mathbf{u} = -\nabla P + \frac{1}{c} (\mathbf{J} \times \mathbf{B})$$

$$\rho \left(\frac{\partial}{\partial t} + \mathbf{u} \cdot \nabla \right) e = -P \nabla \cdot \mathbf{u} + \frac{1}{\sigma} \mathbf{J}^2$$

$$\frac{\partial \mathbf{B}}{\partial t} = \nabla \times (\mathbf{u} \times \mathbf{B}) - \nabla \times \left(\frac{c^2}{4\pi\sigma} \nabla \times \mathbf{B} \right)$$

$$\nabla \cdot \mathbf{B} = 0 \quad P = P(\rho, e) \quad \nabla \times \mathbf{H} = \frac{4\pi}{c} \mathbf{J} \quad \mathbf{H} = \mu \mathbf{B}$$

Constant in time magnetic field approximation

For low magnetic Reynolds number MHD flows, we can neglect the influence of the induced magnetic field. We assume that \mathbf{B} is constant and given as an external field. The electric field is a potential vector field.

The distribution of currents can be found by solving Poisson's equation:

$$\mathbf{J} = \sigma \left(-\nabla \phi + \frac{1}{c} \mathbf{u} \times \mathbf{B} \right)$$

$$\Delta \phi = \frac{1}{c} \nabla \cdot (\mathbf{u} \times \mathbf{B}),$$

with $\left. \frac{\partial \phi}{\partial \mathbf{n}} \right|_{\Gamma} = \frac{1}{c} (\mathbf{u} \times \mathbf{B}) \cdot \mathbf{n}$

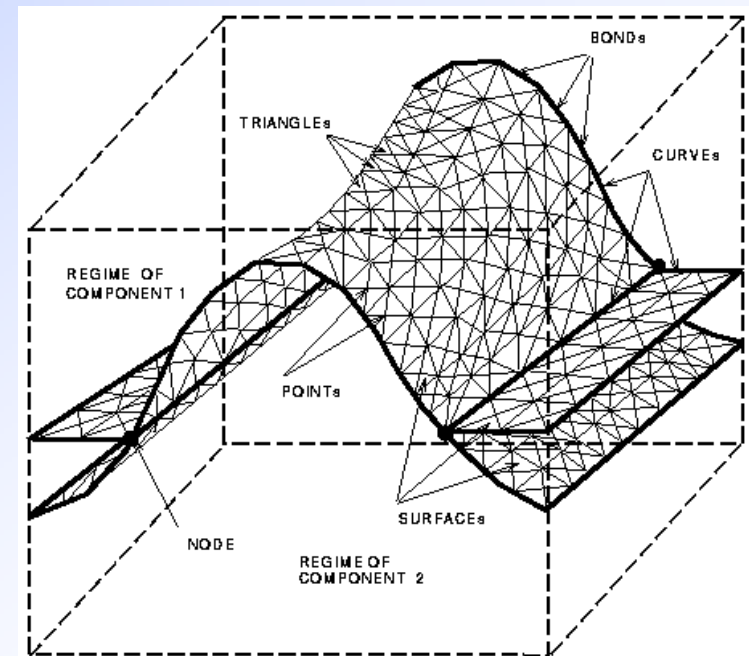
Numerical Approach: Operator Splitting

- The hyperbolic subsystem is solved on a finite difference grid in both domains separated by the free surface using FronTier's interface tracking numerical techniques. The evolution of the free fluid surface is obtained through the solution of the Riemann problem for compressible fluids.
- The parabolic or elliptic subsystem is solved using a finite element method. The grid is dynamically rebuilt and conformed to the evolving interface.

Numerical methods for the hyperbolic subsystem implemented in the *FronTier* Code

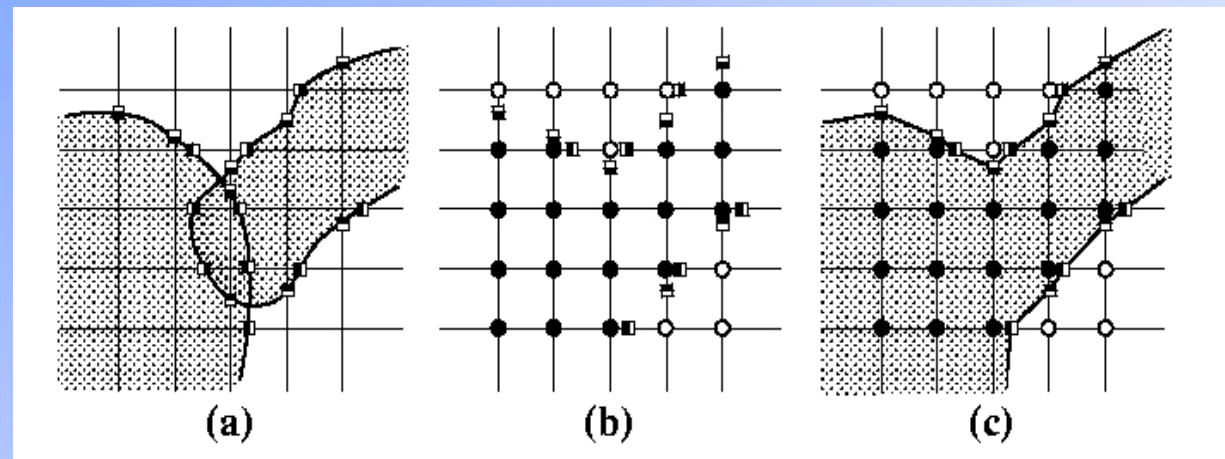
- The FronTier code is based on front tracking. Conservative scheme.
- Front tracking features include the absence of the numerical diffusion across interfaces. It is ideal for problems with strong discontinuities.
- Away from interfaces, FronTier uses high resolution (shock capturing) methods
- FronTier uses realistic EOS models:
 - SESAME
 - Phase transition (cavitation) support

Brookhaven Science Associates
U.S. Department of Energy



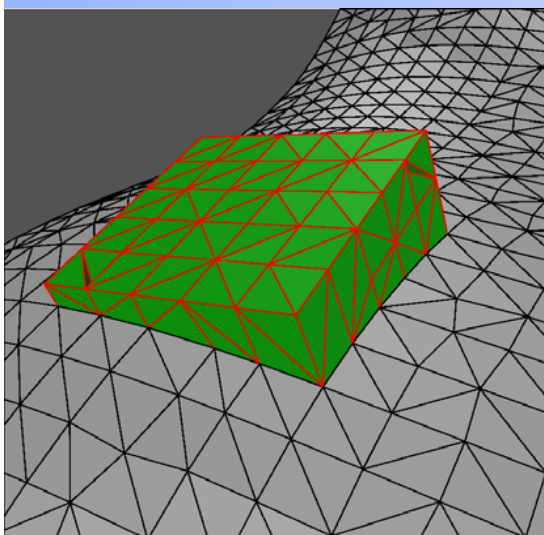
Hyperbolic step:

- Propagate interface
- Resolve interface tangling using grid based method
- Update interior states



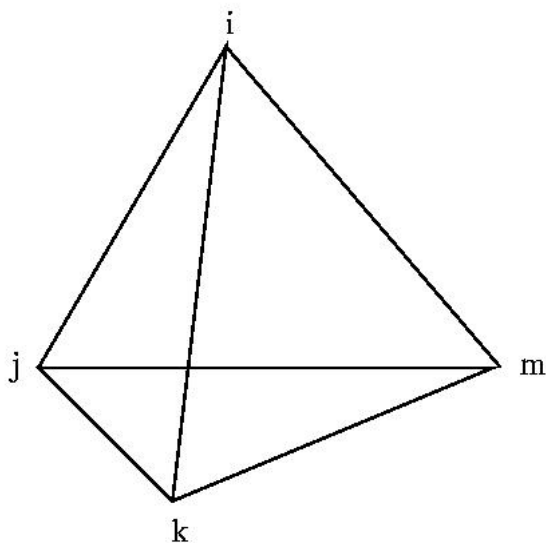
Elliptic/parabolic step:

- Construct FE grid using FD grid and interface data
or
Use the embedded boundary technique
- Solve elliptic/parabolic problem
- Update interior states



Triangulated tracked surface and tetrahedralized hexahedra conforming to the surface. For clarity, only a limited number of hexahedra have been displayed.

Special (div or curl free) basis functions for finite element discretization. Example: Whitney elements



Let λ_i be a barycentric function of the node i with the coordinates x_i

Whitney elements of degree 0 or “nodal elements”:

$$w_{ij}^n = \lambda_i$$

Whitney elements of degree 1 or “edge elements”:

$$w_{ij}^e = \lambda_i \nabla \lambda_j - \lambda_j \nabla \lambda_i$$

Whitney elements of degree 2 or “facet elements”:

$$w_{ijk}^f = 2(\lambda_i \nabla \lambda_j \times \nabla \lambda_k + \lambda_j \nabla \lambda_k \times \nabla \lambda_i + \lambda_k \nabla \lambda_i \times \nabla \lambda_j)$$

Elliptic/Parabolic Solvers

- Instead of solving the Poisson equation, $\Delta\phi = \frac{1}{c}\nabla(\mathbf{u} \times \mathbf{B})$ + Neumann B.C.

we solve $\nabla \cdot \mathbf{E} = \frac{1}{c}(\mathbf{u} \times \mathbf{B})$

$$\mathbf{E} = -\nabla\phi$$

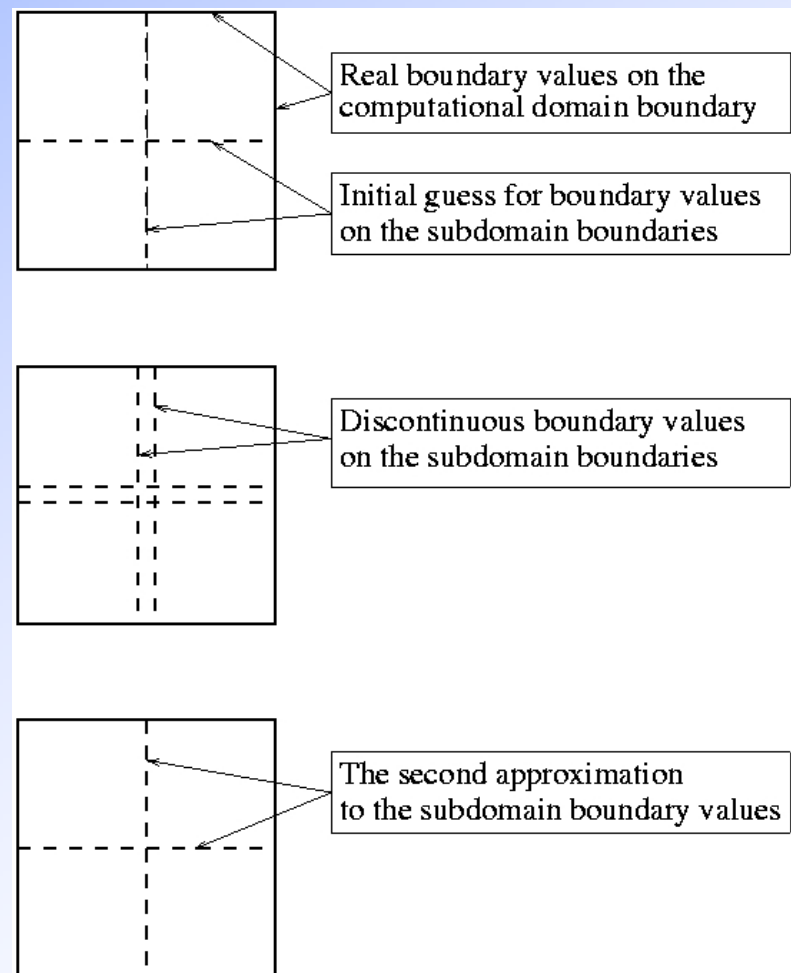
for achieving better accuracy and local conservation.

- High performance parallel elliptic solvers based on Krylov subspace methods (PETSc package) and multigrid solvers (HYPRE package).

Parallelization for distributed memory machines

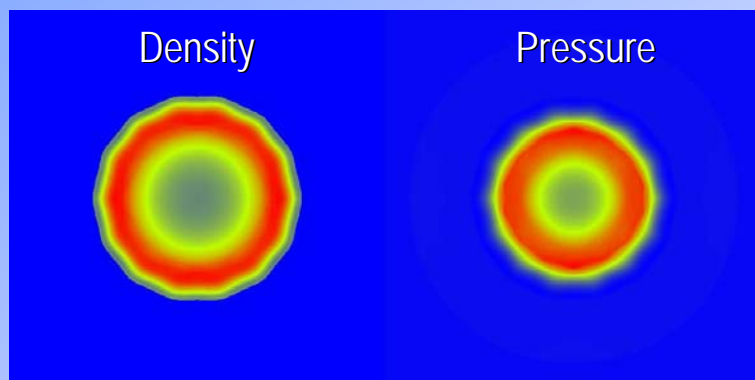
- Hyperbolic solver: overlapping domain decomposition. Processors interchange interior states and interface data of the overlapping region

- Elliptic solver: non-overlapping domain decomposition. Linear systems in subdomains are solved using direct methods and the global wire basket problem is solved iteratively.

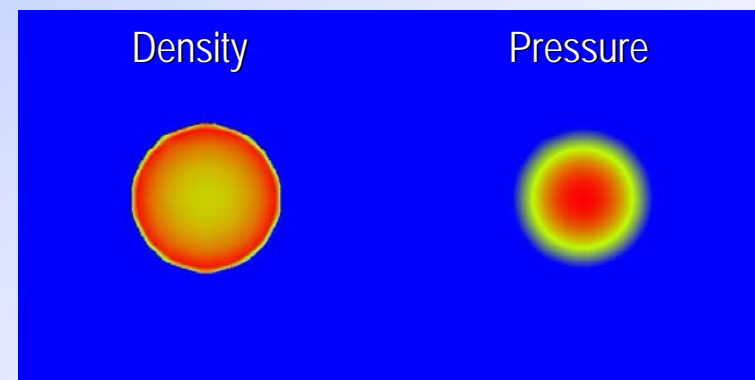


Numerical example: propagation of shock waves due to external energy deposition

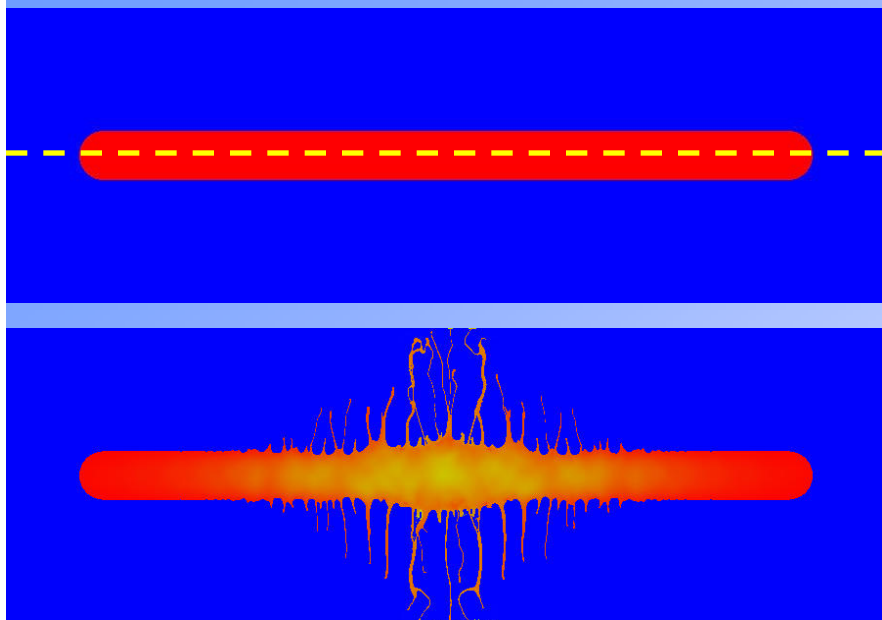
Evolution of a hydro shock.



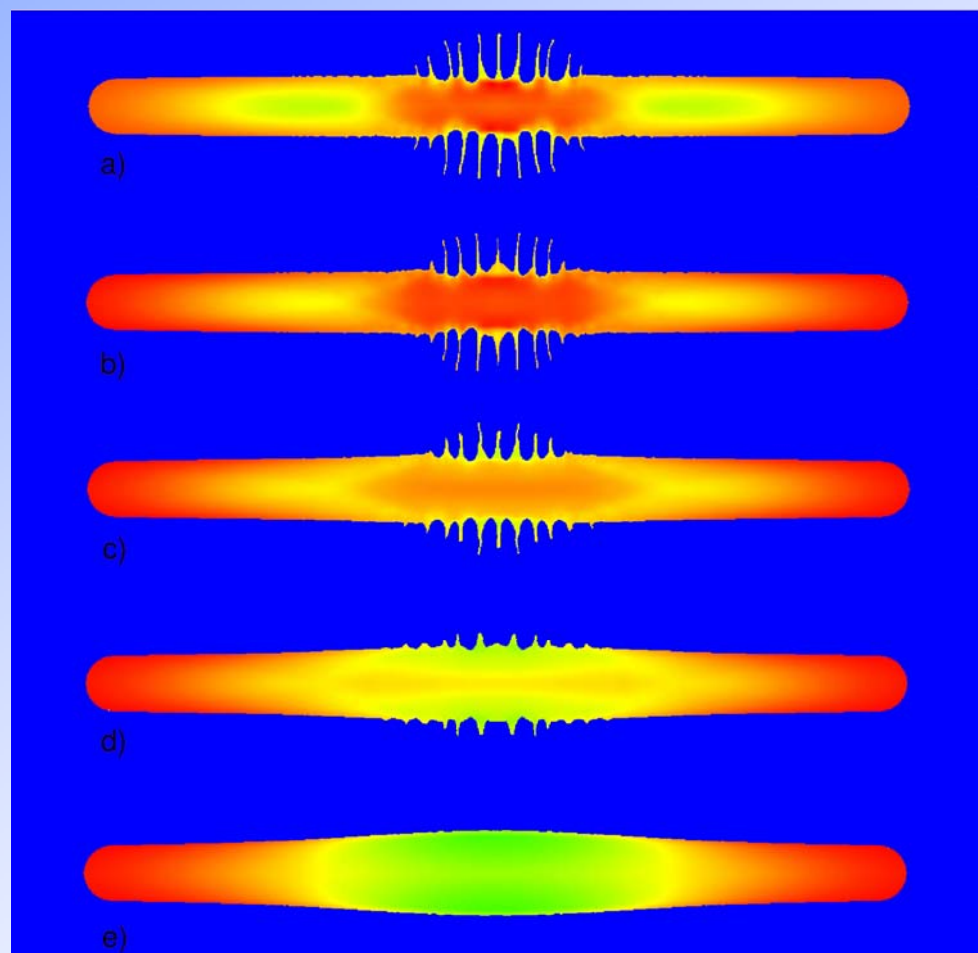
MHD effects reduce the velocity of the shock and the impact of the energy deposition.



Richtmyer-Meshkov instability and MHD stabilization

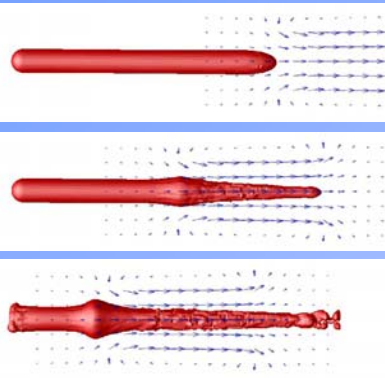


Simulation of the mercury jet
– proton pulse interaction
during 100 microseconds,
 $B = 0$

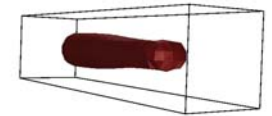


a) $B = 0$ b) $B = 2T$ c) $B = 4T$
d) $B = 6T$ e) $B = 10T$

Other applications



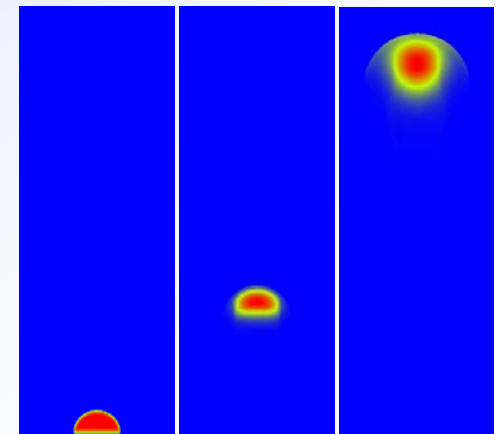
Conducting liquid jets in longitudinal and transverse magnetic fields. Left: Liquid metal jet in a 20 T solenoid. Right: Distortion (dipole and quadruple deformations) of a liquid metal jet in a transverse magnetic field. Benchmark problem: Sandia experiments for AIPLEX project, experiments by Oshima and Yamane (Japan).



Laser ablation plasma plumes. Plasma plumes created by pulsed intensive laser beams can be used in a variety of technological processes including the growth of carbon nanotubes and high-temperature superconducting thin films.

Our future goal is to control the plasma expansion by magnetic fields.

Numerical simulation of laser ablation plasma plume



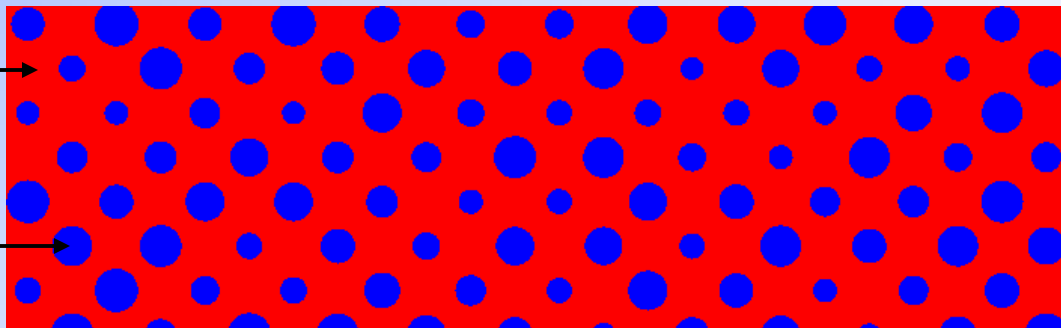
Equation of state modeling and the problem of cavitation

- The strength of rarefaction waves in mercury targets significantly exceeds the mercury cavitation threshold. The dynamics of waves is significantly different in the case of cavitating flows.
- The use of one-phase stiffened polytropic EOS for liquid in the mercury jet target simulations led to much shorter time scale dynamics and did not reproduce experimental results at low energies.
- To resolve this problem, we have been working on direct and continuous homogeneous EOS models for cavitating and bubbly flows.

EOS for cavitating and bubbly fluids: two approaches

- **Direct method:** Each individual bubble is explicitly resolved using FronTier interface tracking technique.

Stiffened polytropic EOS for liquid



Polytropic EOS for gas (vapor)

- **Homogeneous EOS model.** Suitable average properties are determined and the mixture is treated as a pseudofluid that obeys an equation of single-component flow.

Direct method: Pro and Contra

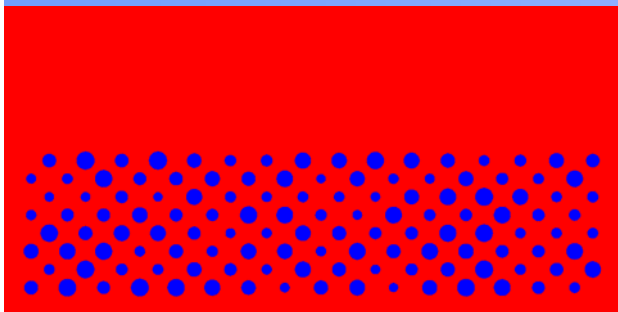
Advantages:

- Accurate description of multiphase systems limited only to numerical errors.
- Accurate treatment of drag, surface tension, viscous, and thermal effects. More easy to account for the mass transfer due to phase transition.
- Discontinuities of physical properties are also beneficial for MHD.

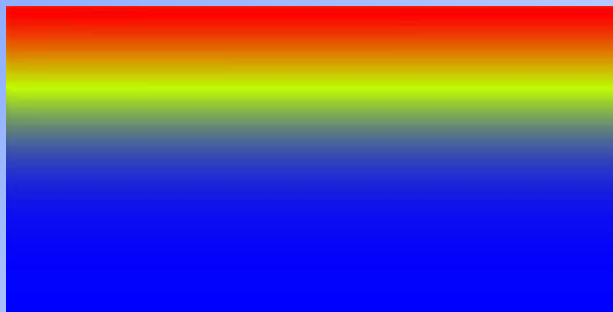
Disadvantages:

- Very complex and computationally expensive, especially in 3D.
- Designed only for FronTier. Impossible to create a general purpose EOS library.

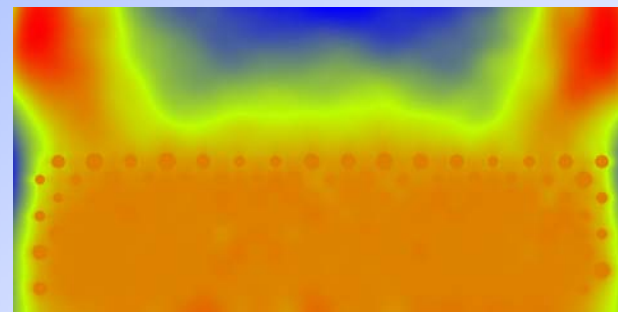
Numerical example: strong wave in bubbly liquid



a)



b)

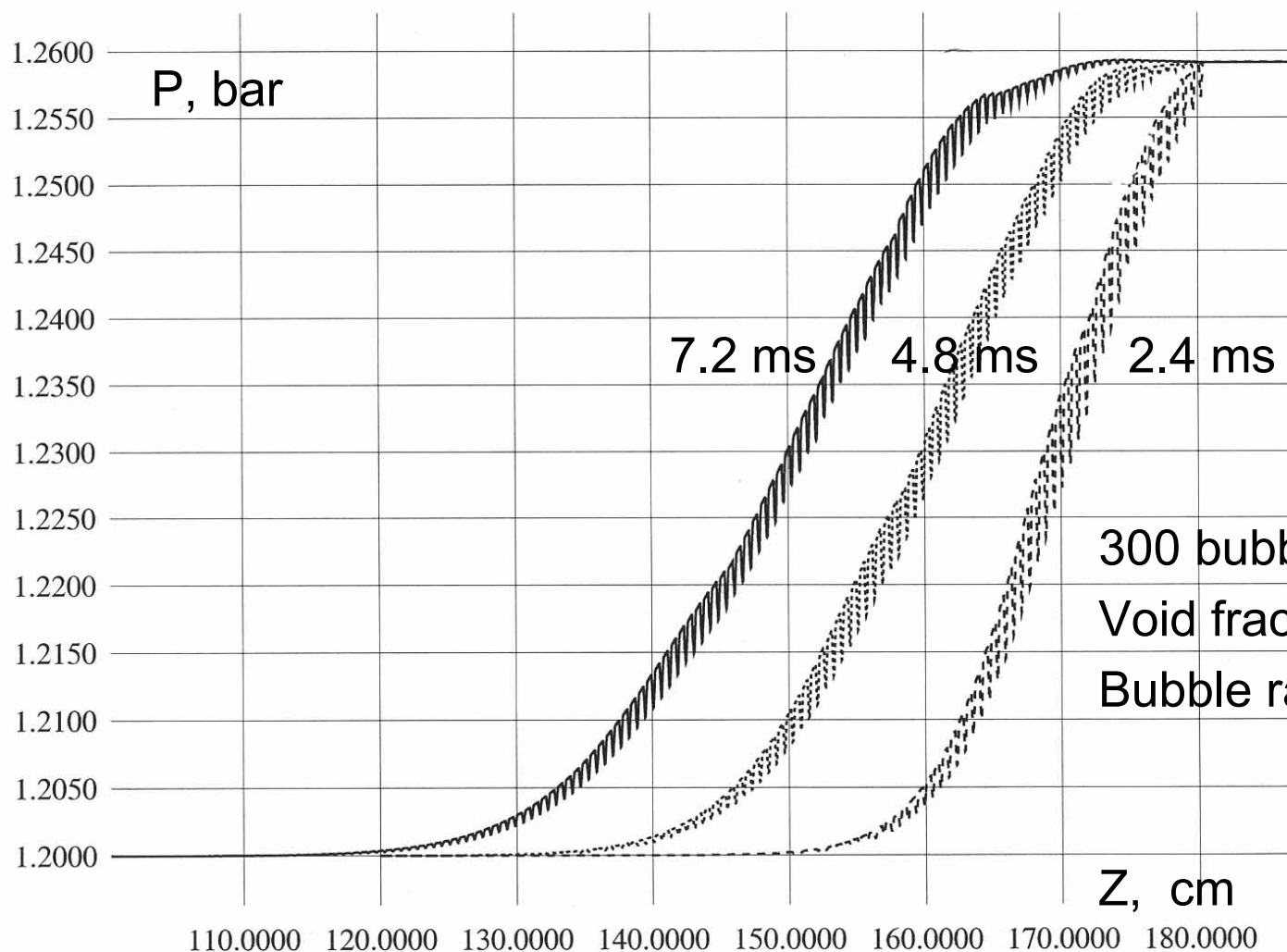


c)

Direct numerical simulation of the pressure wave propagation in a bubbly liquid: a) initial density; red: mercury, blue: gas bubbles, b) initial pressure; the pressure is 500 bar at the top and 1 bar at the bottom, c) pressure distribution at time 100 microseconds; pressure is 6 bar at the bottom.

Current problem: develop a nonlocal Riemann solver for the propagation of free interfaces which takes into account the mass transfer due to phase transitions.

Direct simulation of classical shock tube experiments in air bubble – water mixture



300 bubbles in the layer.
Void fraction is 2.94%
Bubble radius is 1.18 mm

Continuum homogeneous EOS models

- A simple isentropic EOS for two phase fluid.
- EOS based on Rayleigh-Plesset type equations for the evolution of an average bubble size distribution.
- Range of applicability for linear and non-linear waves.
- Benchmark problems

Equation of state

An EOS is a relation expressing the specific internal energy E of a material as a function of the entropy S and the specific volume V : $E(S, V)$.

The pressure P and temperature T are first derivatives of the energy E :

$$P(V, S) = -\left.\frac{\partial E}{\partial V}\right|_S, \quad T(V, S) = \left.\frac{\partial E}{\partial S}\right|_V$$

in accordance with the second law of thermodynamics: $TdS=dE+PdV$.

The second derivatives of the internal energy are related to the adiabatic exponent γ , the Gruneisen coefficient Γ and the specific heat g .

Thermodynamic constraints

Thermodynamic constraints:

- $E = E(S, V)$ is continuously differentiable and piecewise twice continuously differentiable.
- $T \geq 0, \quad P \geq 0.$
- E is jointly convex as a function of V and S . This translates into the inequalities $g \geq 0, \quad \gamma \geq 0 \quad \text{and} \quad \gamma g \geq \Gamma^2,$

Or equivalently $C_V^{-1} \geq C_P^{-1} \geq 0 \quad \text{and} \quad K_S^{-1} \geq K_T^{-1} \geq 0.$

- Asymptotic constraints:
- $P(V, S) \rightarrow \infty \quad \text{as} \quad V \rightarrow 0.$
 - $P(V, S) \rightarrow 0 \quad \text{as} \quad V \rightarrow \infty.$
 - $E(V, S) \rightarrow \infty \quad \text{and} \quad P(V, S) \rightarrow \infty \quad \text{as} \quad S \rightarrow \infty.$

Analytical model: Isentropic EOS for two phase flow

- A thermodynamically consistent connection of three branches describing mixture, and pure liquid and vapor phases. Isentropic approximation reduces a thermodynamic state to one independent variable (density).
- Gas (vapor) phase is described by the polytropic EOS reduced to an isentrope.

$$P = (\gamma_0 - 1)E\rho,$$

$$T = \frac{P}{R\rho},$$

$$S = (\log P - \gamma_0 \log \rho) \frac{R}{\gamma_0 - 1}.$$

$$S = \text{const} \Rightarrow$$

$$P = \eta\rho^\gamma, \quad E = \frac{\eta}{\gamma - 1} \rho^{\gamma-1}, \quad T = \frac{\eta}{R} \rho^{\gamma-1},$$

$$\text{where } \eta = \exp\left(\frac{S(\gamma - 1)}{R}\right)$$

The mixed phase

- The mixed phase is described as follows:

$$P(\rho) = P_l^{sat} + P_{vl} \log \left[\frac{\rho_v a_v^2 (\rho_l + \alpha (\rho_v - \rho_l))}{\rho_l (\rho_v a_v^2 - \alpha (\rho_v a_v^2 - \rho_l a_l^2))} \right],$$

$$E(\rho) = \int_{\rho_v^{sat}}^{\rho} \frac{P}{\rho^2} d\xi,$$

where

$$P_{vl} = \frac{\rho_v a_v^2 \rho_l a_l^2 (\rho_v - \rho_l)}{\rho_v^2 a_v^2 - \rho_l^2 a_l^2},$$

and α is the void fraction: $\alpha = \frac{\rho - \rho_l}{\rho_v - \rho_l}$.

The liquid phase

- The liquid phase is described by the stiffened polytropic EOS:

$$P = (\gamma - 1)\rho(E + E_\infty) - \gamma P_\infty,$$

$$T = \frac{P + P_\infty}{R\rho},$$

$$S = (\log(P + P_\infty) - \gamma_0 \log \rho) \frac{R}{\gamma_0 - 1}.$$

$$S = \text{const} \Rightarrow$$

$$P = \eta \rho^\gamma - P_\infty,$$

$$E = \frac{\eta}{\gamma - 1} \rho^{\gamma-1} + \frac{P_\infty}{\rho} - E_\infty, \quad T = \frac{\eta}{R} \rho^{\gamma-1},$$

$$\text{where } \eta = \exp\left(\frac{S(\gamma - 1)}{R}\right)$$

Features of the isentropic EOS model

- The most important feature is correct dependence of the sound speed on the density (void fraction).
- Enough input parameters (thermodynamic/acoustic parameters of both saturated points) to fit the sound speed to experimental data.
- Absence of drag, surface tension, and viscous forces. Incomplete thermodynamics (isentropic approximation). No any features of bubble dynamics.
- Despite simplicity, the EOS led to significant improvements in modeling of the mercury – proton pulse interaction.

EOS models based on Rayleigh-Plesset equation

A dynamic closure for fluid dynamic equations can be obtained using Rayleigh-Plesset type equations for the evolution of an average bubble size distribution

$$RR_{tt} + \frac{3}{2}(R_t)^2 + \delta_D \frac{1}{R} R_t + \frac{2}{We} \left[\frac{1}{R} - \frac{1}{R^{3\gamma}} \right] + \frac{\sigma}{2} \left[1 - \frac{1}{R^{3\gamma}} \right] + C_p = 0,$$

where

δ_D is the effective damping coefficient

We is the Weber number

σ is the cavitation number

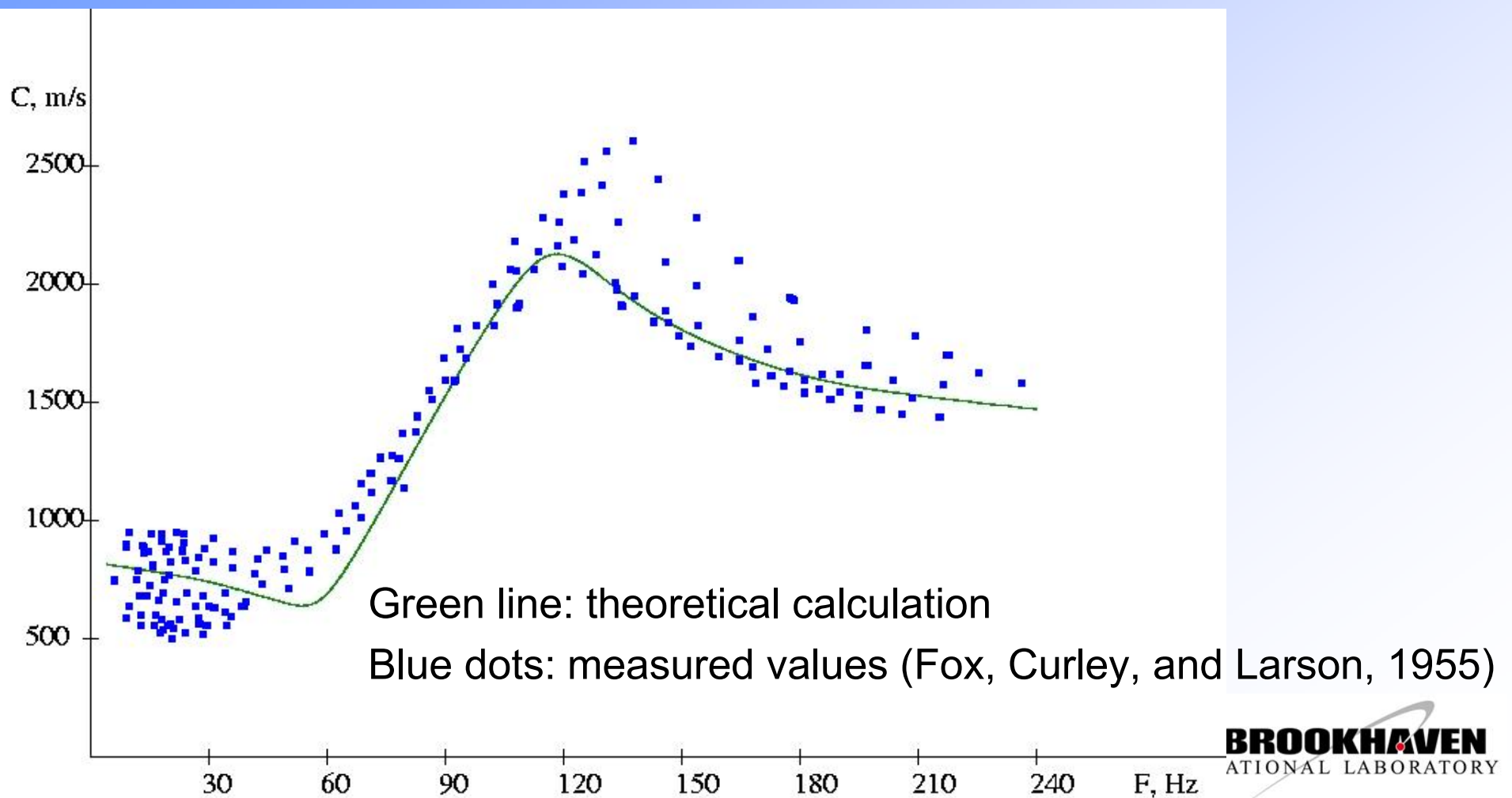
C_p is the pressure term

- EOS includes implicitly drag, surface tension, and viscous forces.

Sound speed in air bubble – water mixture as a function of frequency.

Void fraction is $2.0 \cdot 10^{-4}$

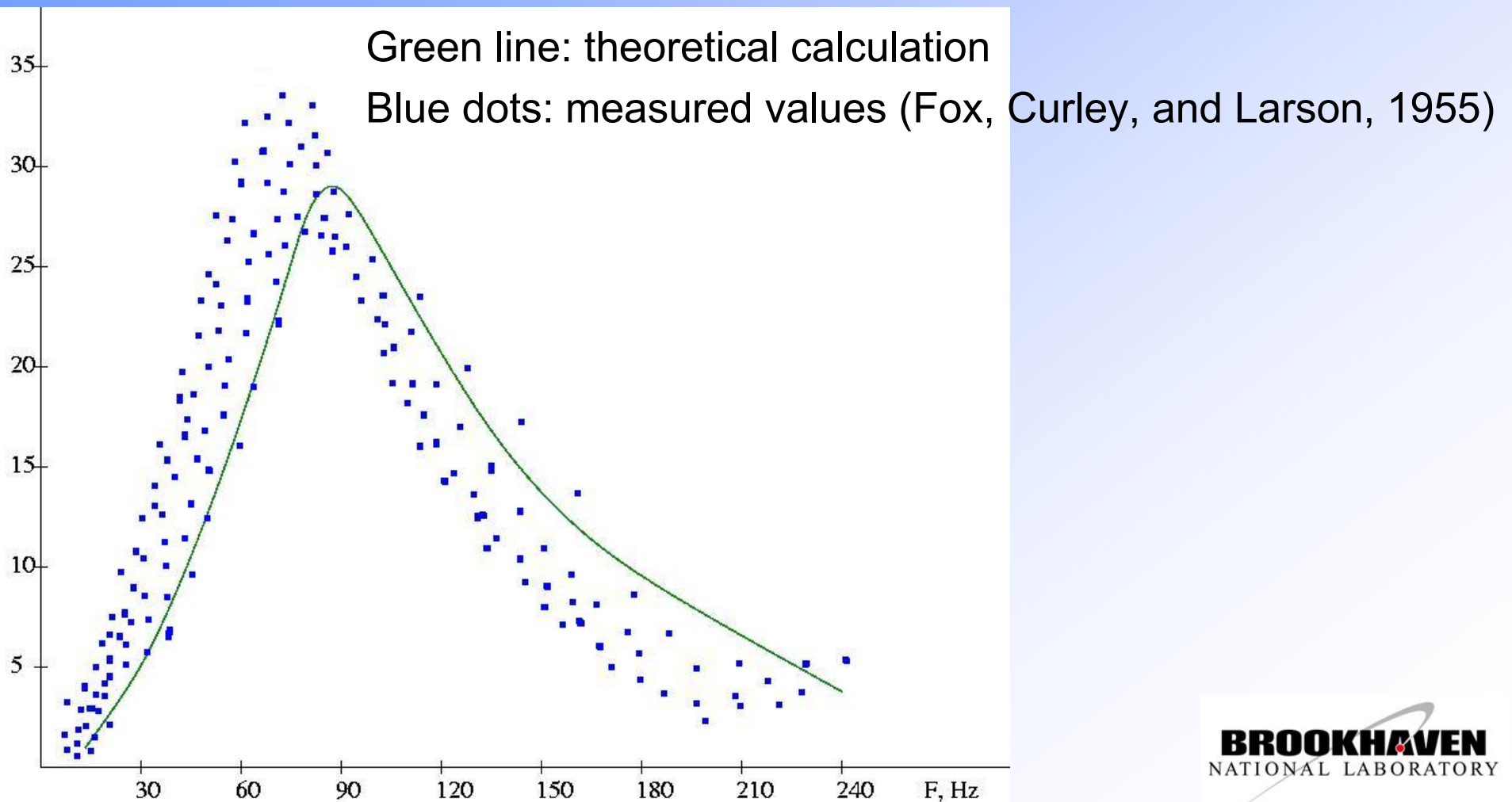
Bubble radius is $(1.2 \pm 0.4) \cdot 10^{-4}$ m



Attenuation of pressure waves in air bubble – water mixture as a function of frequency.

Void fraction is $2.0 \cdot 10^{-4}$

Bubble radius is $(1.2 \pm 0.4) \cdot 10^{-4}$ m

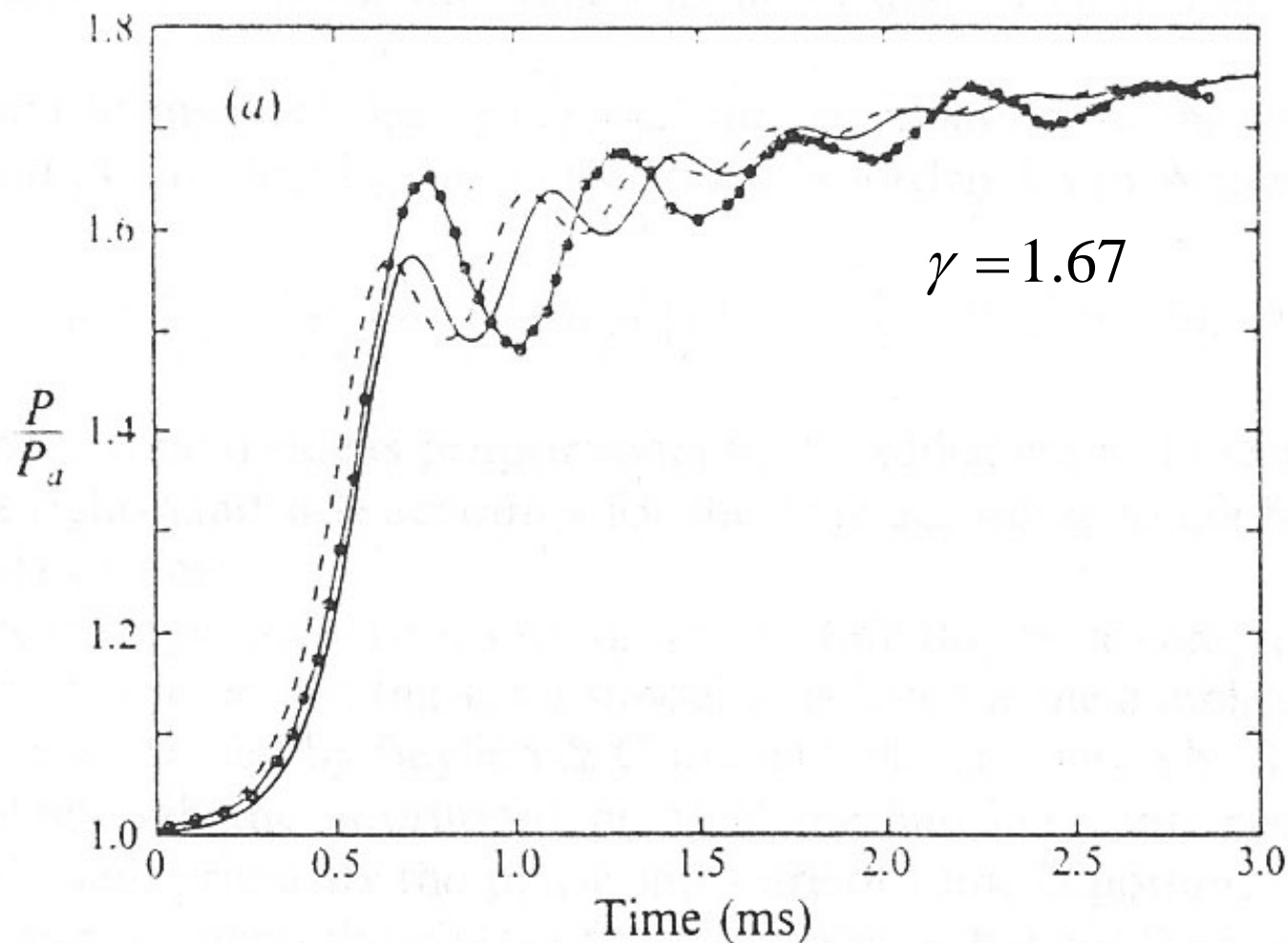


Nonlinear waves: shock-tube experiments with helium bubbles

Solid and dashed lines: theoretical calculation (Wanatabe and Prosperetti, 1994)

Dots: measured values (Beylich and Gulhan, 1990)

Void fraction is 0.25% and bubble radius is 1.15 mm

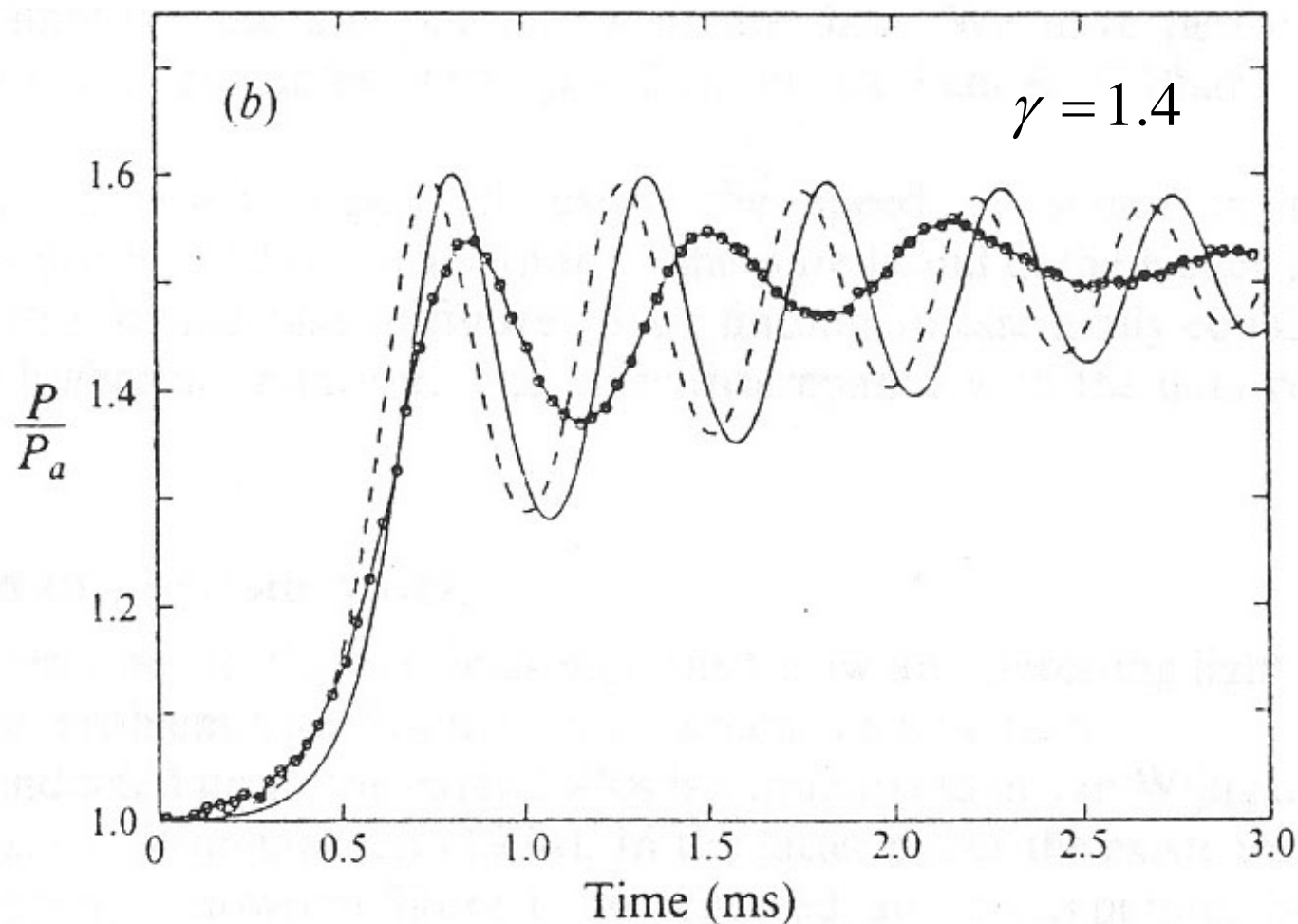


Nonlinear waves: shock-tube experiments with nitrogen bubbles

Solid and dashed lines: theoretical calculation (Wanatabe and Prosperetti, 1994)

Dots: measured values (Beylich and Gulhan, 1990)

Void fraction is 0.25% and bubble radius is 1.15 mm

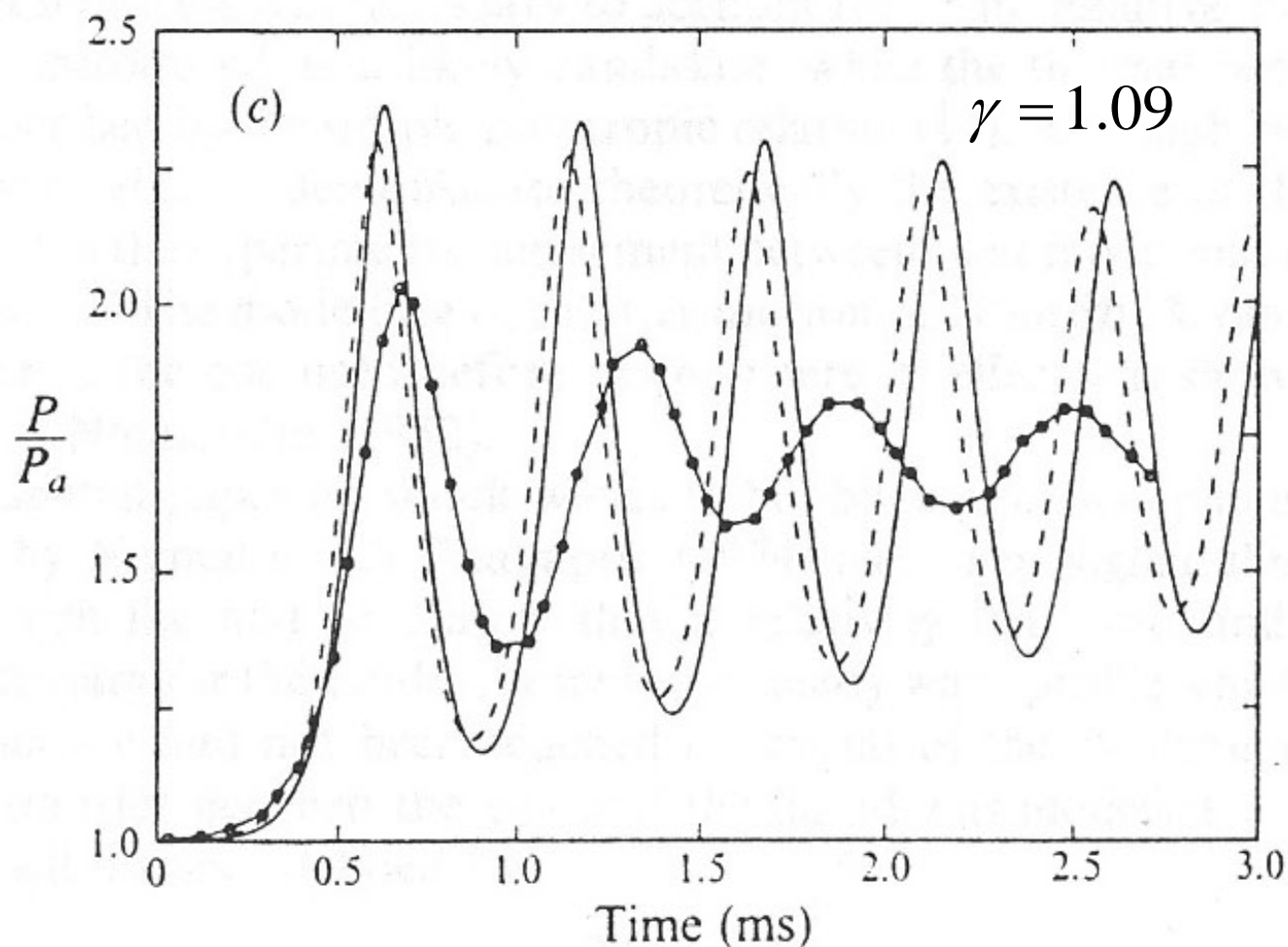


Nonlinear waves: shock-tube experiments with SF₆ bubbles

Solid and dashed lines: theoretical calculation (Wanatabe and Prosperetti, 1994)

Dots: measured values (Beylich and Gulhan, 1990)

Void fraction is 0.25% and bubble radius is 1.15 mm



Current and Future research

- Development of a Riemann solver with the Alfvén wave support
- Development of a Riemann solver accounting for mass transfer due to phase transitions
- Further work on the EOS modeling for cavitating and bubbly flows.
- Further studies of the muon collider target issues. Studies of the cavitation phenomena in a magnetic field.
- Studies of hydrodynamic issues of the cavitation induced erosion in the SNS target.
- Studies of the MHD processes in liquid lithium jets in magnetic fields related to the APEX experiments.
- Studies of the dynamics of laser ablation plumes in magnetic fields.